

Dessins d'Enfants in $\mathcal{N} = 2$ Generalised Quiver Theories

Yang-Hui He¹ and James Read²

¹*Department of Mathematics, City University, London,
Northampton Square, London EC1V 0HB, UK;
School of Physics, NanKai University, Tianjin, 300071, P.R. China;
Merton College, University of Oxford, OX1 4JD, UK
hey@maths.ox.ac.uk*

²*Merton College, University of Oxford, OX1 4JD, UK
james.read@merton.ox.ac.uk*

Abstract

We study Grothendieck's *dessins d'enfants* in the context of the $\mathcal{N} = 2$ supersymmetric gauge theories in $(3 + 1)$ dimensions with product $SU(2)$ gauge groups which have recently been considered by Gaiotto *et al.* We identify the precise context in which dessins arise in these theories: they are the so-called ribbon graphs of such theories at certain isolated points in the moduli space. With this point in mind, we highlight connections to other work on trivalent dessins, gauge theories, and the modular group.

Contents

1	Introduction	3
2	Dramatis Personæ	6
2.1	Skeleton Diagrams	6
2.2	Moduli Spaces	8
2.3	BPS Quivers	9
2.4	Quadratic Differentials and Graphs on Gaiotto Curves	11
2.5	Dessins d’Enfants and Belyi Maps	12
2.6	The Modular Group and Congruence Subgroups	14
3	A Web of Correspondences	15
3.1	Quadratic Differentials and Seiberg-Witten Curves	16
3.2	Trajectories on Riemann Surfaces and Ideal Triangulations	16
3.3	Constructing BPS Quivers	20
3.4	Skeleton Diagrams and BPS Quivers	21
3.5	Strebel Differentials and Ribbon Graphs	23
3.5.1	Ribbon Graphs from Strebel Differentials	23
3.5.2	Ribbon Graphs as Dessins	24
3.5.3	Strebel Differentials from Belyi Maps	25

3.5.4	Enumerating Ribbon Graphs	26
3.5.5	Connections to Modularity	27
3.5.6	Location of the Strebel Points in the Coulomb Branch	29
3.5.7	Dessins at Other Points in the Moduli Space	29
3.5.8	Further Conjectures	31
3.6	Taking Stock	34
4	Skeleton Diagrams to Seiberg-Witten Curves: An Alternative Route?	35
5	Conclusions and Outlook	39

1 Introduction

In the mid-1990s, the pioneering work of Seiberg and Witten [1] led to a revolution in the study of $\mathcal{N} = 2$ supersymmetric gauge theories in $(3 + 1)$ dimensions. Their work, which has come to be known as Seiberg-Witten theory, deals with the construction of the non-perturbative dynamics of $\mathcal{N} = 2$ theories in the limit of low energy and momenta. The jewel in the crown of Seiberg-Witten theory is the **Seiberg-Witten curve**: a (hyper)elliptic curve, the periods of which completely specify the spectra, coupling, and low-energy effective Lagrangian, as well as non-perturbative information of the gauge theory.

In this paper, we undertake a study of a class of $\mathcal{N} = 2$ theories known as **Gaiotto theories**. These theories have interesting duality behaviour amongst themselves under S-duality and possess a systematic string-theoretic construction for their Seiberg-Witten curves [2]: take a Riemann surface \mathcal{C} of genus g with n punctures, dubbed the **Gaiotto curve**, and wrap N coincident parallel M5-branes over it. The world-volume theory on the M5-brane is one with a product $SU(N)$ group, the Seiberg-Witten curve for which



Figure 1: (a) Skeleton diagram and (b) BPS quiver for the Gaiotto theory with a single $SU(2)$ factor and $N_f = 4$.

is an N -fold cover over \mathcal{C} .

Let us henceforth take $N = 2$. Each such Gaiotto theory has a product $SU(2)^{3g-3+n}$ gauge group [3], and all can be encoded into a **skeleton diagram**, also known as a **generalised quiver diagram** [3]. This is a trivalent graph with internal edges corresponding to $SU(2)$ groups and external legs corresponding to flavours. Hence we have a graph with g closed circuits, $3g - 3 + n$ edges, $2g - 2 + n$ nodes, and n external lines. The diagram constitutes the spine of the amoeba projection of the Gaiotto curve [4], and hence captures the genus and number of punctures on \mathcal{C} . Each skeleton diagram determines a unique $(3 + 1)$ dimensional $\mathcal{N} = 2$ gauge theory [2].

To illustrate, the skeleton diagram for the Gaiotto theory with a single $SU(2)$ factor and $N_f = 4$ flavours (which, in virtue of its simplicity, we shall use as a running example) is shown in Figure 1(a). Note that in this paper, N_f always denotes the number of $SU(2)$ factors in the flavour symmetry group, rather than the number of so-called *fundamental flavours* which appear in the linear quivers drawn in e.g. [5, 6]. The corresponding *BPS quiver*, to be discussed below, is drawn in Figure 1(b).

In a parallel vein, the Seiberg-Witten curves for $SU(2)$ Gaiotto theories can be written in the form $y^2 = \phi(x)$, where $q = \phi(x) dx^2$ is a **quadratic differential** on \mathcal{C} with only second order poles [5, 7]. The functional form of q is specified by the topology $\langle g, n \rangle$ of the skeleton; varying individual parameters in q amounts to changing the point in the moduli space of the theory under consideration. With this in mind, an obvious question now arises: given a specific skeleton diagram, how do we extract the relevant Seiberg-Witten curve for that Gaiotto theory, as well as other information about the theory, such as that relating to its BPS spectrum?

Though the answer to this question turns out to be simple, consideration as to how to respond leads us to an intricate web of recently-discovered structures important in the study of $SU(2)$ Gaiotto theories. In addition to the structures introduced above, this web includes the so-called **BPS quivers** which arise in the BPS spectroscopy of the theory, in addition to several important graphs drawn on \mathcal{C} . Many of the structures in this web have already been carefully elaborated in the recent work on BPS quivers in the context of Gaiotto theories (see [7–9]), and in other work on Gaiotto theories ([2, 3, 5], etc.). By presenting this web, we are able to precisely identify where **dessins d’enfants**, i.e. bipartite graphs drawn on Riemann surfaces, arise in the context of these Gaiotto theories, thereby in turn allowing us to connect the study of $SU(2)$ Gaiotto theories to previous work on dessins in the context of $\mathcal{N} = 2$ theories [2, 10, 11].

Specifically, it turns out that dessins arise in the context of these theories as so-called **ribbon graphs** on \mathcal{C} , at isolated points in the Coulomb branch of the moduli space where the quadratic differential on \mathcal{C} satisfies the definition of a so-called **Strebel differential**, and further where n additional real numbers associated to the punctures are tuned such that the edges of the ribbon graphs have equal lengths [12]. Recognising this yields many results. First, by **Belyi’s theorem**, we find that Gaiotto curves at such points have the structure of algebraic curves defined over $\overline{\mathbb{Q}}$. Next, results from [12] yield an efficient means of computing the explicit Strebel differentials, and therefore Seiberg-Witten curves, at these points in the moduli space, via the dessin’s associated **Belyi map**. In addition, we are led to connections with the dessins in [13], which correspond to certain subgroups of the modular group, and to conjectures on further connections to the work of [10, 11] on dessins and $\mathcal{N} = 2$, $U(N)$ gauge theories.

With an understanding of all these structures and connections, in particular of the role of dessins in the study of these Gaiotto theories, we proceed in the final part of this paper to study an alternative proposal for the role of dessins in $SU(2)$ Gaiotto theories. Specifically, it has recently been suggested in [2] that the skeleton diagrams themselves can be interpreted as dessins d’enfants, from which one can extract the relevant Seiberg-Witten curve by manipulating the associated Belyi map. We shall show that such a suggestion needs to be modified in general, and shall provide a number of examples to highlight this.

The structure of this paper is as follows. In §2, we introduce all the key structures which arise in the study of $SU(2)$ Gaiotto theories. In §3, we elaborate the connections between these structures, providing an extended discussion of the role of dessins d'enfants in the context of these theories. Finally, in §4 we evaluate the above-mentioned alternative proposals for how dessins arise in the context of these theories.

2 Dramatis Personæ

In this section, we present a pedagogical summary of all the important mathematical structures which arise in the study of $SU(2)$ Gaiotto theories; the web of interrelations between these structures shall then be elaborated in the following section. In §2.1, we present some more technical details on skeleton diagrams. In §2.2, we recall the essential details of the vacuum moduli spaces of $\mathcal{N} = 2$ theories. Next, in §2.3, we remind ourselves of the role of BPS quivers in these theories. In §2.4, we consider many of the important graphs which can be drawn on the Gaiotto curve \mathcal{C} . In §2.5, we introduced a technical definition of dessins d'enfants and the associated Belyi maps. Finally, in §2.6 we introduce the modular group and some important subgroups.

As a prelude to our discussion in §3 of the connections between all these objects, we provide in Figure 2 a roadmap of these connections, to aid orientation in the ensuing discussion. The first half of §3 will focus on the horizontal chain of correspondences shown in Figure 2. Though most of these links have been detailed in the literature previously, it should be useful to present a codified story in one place, with the focus on going from a skeleton diagram to the BPS spectrum and Seiberg-Witten curve of that theory. Doing so will allow us to provide an extended discussion of the role of dessins in these theories; this we shall do in the second half of §3.

2.1 Skeleton Diagrams

In [5], Gaiotto found a new and interesting class of $\mathcal{N} = 2$ supersymmetric gauge theories in $(3 + 1)$ dimensions, obtainable from the wrapping of M5 branes over Riemann

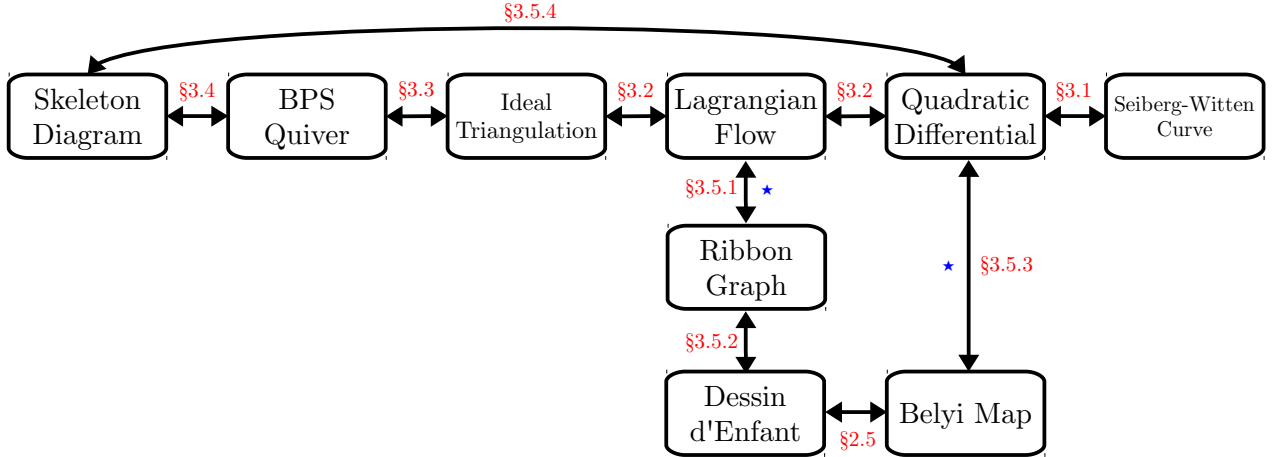


Figure 2: A roadmap to the major connections between the objects of importance in the study of $SU(2)$ Gaiotto theories. Each of the major constructions of importance to $SU(2)$ Gaiotto theories is shown. Arrows represent connections between these entities. The section in which each connection is discussed is indicated in red. Correspondences marked with a blue star hold only when the quadratic differential on \mathcal{C} is a Strebel differential; this shall be explained in §3.

surfaces. Following [3], let us focus on the case where the gauge group is a product of only $SU(2)$ factors. In this case, we can unambiguously represent the relevant gauge theories as so-called **skeleton diagrams**, consisting of lines and trivalent nodes, where a line represents an $SU(2)$ gauge group and a trivalent node represents a matter field in the tri-fundamental representation $SU(2)^3$. Hence, these diagrams can be seen as generalisations of the more familiar **quiver diagrams**, which have arisen both in representation theoretic [14] and gauge theoretic contexts [15]. Indeed, whereas fields charged under *two* SU -factors, being the fundamental under one and the anti-fundamental of another, readily afford description in terms of arrows in a quiver, fields charged under more than two factors, as in our present case, require encoding beyond a quiver diagram.

Our skeleton diagrams are straightforward: they give rise to an infinite class of $\mathcal{N} = 2$ gauge theories, having each line representing an $SU(2)$ gauge group with its length inversely proportional to its gauge coupling g_{YM}^2 and each trivalent node representing a half-hypermultiplet $Q_{\alpha\beta\gamma}$ transforming under the tri-fundamental $(\square, \square, \square)$ representation of $SU(2) \times SU(2) \times SU(2)$ with $\alpha, \beta, \gamma = 1, 2$ indexing each of the $SU(2)$ factors. Any line of infinite length gives zero coupling and the associated $SU(2)$ factor becomes

a global flavour symmetry. Because $\mathcal{N} = 2$ supersymmetry is large enough to have its matter content determine the interactions completely, each skeleton diagram thus defines a unique $(3 + 1)$ -dimensional $\mathcal{N} = 2$ gauge theory. Any legitimate skeleton diagram can be constructed simply through gluing together trivalent vertices.

The string-theoretic realisation of $\mathcal{N} = 2$ Gaiotto theories is in terms of a stack of M5 branes (for our $SU(2)$ Gaiotto theories, we have two M5 branes) wrapping a Riemann surface \mathcal{C} of genus g with n punctures. More precisely, consider M-theory in eleven dimensions with coordinates $x^{0,\dots,10}$ with $x^{7,8,9} = 0$ fixed and $x^{0,1,2,3}$ the coordinates of our four-dimensional world $\mathbb{R}_{x^{0,1,2,3}}^4$. Of the remaining four directions, $Q_{x^{4,5,6,10}} \simeq \mathbb{R}^3 \times \mathbb{R}$, define a complex structure $v = x^4 + ix^5$ and $t = \exp(-x^6 + ix^{10})/R_{IIA}$ (so that the x^{10} direction indeed becomes periodic when compactifying to type IIA string theory on a circle of radius R_{IIA}), and define a Riemann surface $\mathcal{C} = \{F(v, t) = 0\} \subset Q$ over which the M5 brane can wrap. In the type IIA perspective, this corresponds to $n + 1$ NS5-branes occupying $x^{0,1,\dots,5}$ and placed in parallel at fixed values of x^6 ; moreover, between adjacent pairs of NS5-branes are stretched stacks of D4-branes. The variable names are chosen judiciously: the skeleton diagram of the theory to which \mathcal{C} corresponds is one whose topology, graphically, consists of g independent closed circuits and n external (semi-infinite) legs.

We can easily check [3] that given a skeleton diagram specified by the pair $\langle g, n \rangle$, the number of internal (finite) lines, hence the number of $SU(2)$ gauge group factors, is $3g - 3 + n$, while the number of nodes, hence the number of matter fields, is the Euler characteristic $2g - 2 + n$. The Coulomb branch of the moduli space of the Gaiotto theory in question (to be discussed in more depth below) is specified by the topology $\langle g, n \rangle$ of the skeleton diagram [2, 3]. Finally, it is worth noting that the only features of the skeleton diagrams of these theories relevant to the physics they encode are the parameters g and n : this is sometimes referred to as **Gaiotto duality** [9].

2.2 Moduli Spaces

For $\mathcal{N} = 2$ theories, the space of vacuum expectation values of the theory is known as the vacuum **moduli space** of the theory. One can think of this as the space of

minima of an effective potential, governed by the zero loci of a set of algebraic equations. Thus the moduli space is an *affine algebraic variety* on a complex space \mathbb{C}^k , whose coordinates are the vacuum expectation values. As a variety, the moduli space of an $\mathcal{N} = 2$ theory typically decomposes into two *branches*, known as the *Higgs branch* \mathcal{B} and *Coulomb branch* \mathcal{U} . The former is parameterised by the massless gauge singlets of the hypermultiplets, occurring where the gauge group is completely broken and the vector multiplet becomes massive via the Higgs mechanism. The latter is parameterised by the complex scalars in the vector multiplet, occurring when the gauge group is broken to some Abelian subgroup and the hypermultiplets generically become massive.

Though our focus in this paper will mostly be on the Coulomb branch \mathcal{U} , it is worth noting at this point that for $g > 0$, where there is more than a single $SU(N)$ factor, the gauge group may not be completely broken on the Higgs branch of each factor and thus to avoid confusion, the authors of [3] dub this quasi-Higgs branch the *Kibble branch* \mathcal{K} . A beautiful result of [3] is that the Kibble branch of the moduli space is an algebraic variety such that

$$\dim_{\mathbb{H}}(\mathcal{K}) = n + 1, \tag{2.1}$$

where $\dim_{\mathbb{H}}$ means the *quaternionic* dimension, i.e. four times the real dimension or twice the complex dimension. It is interesting to see that this result is independent of g . A quick argument would proceed as follows: each trivalent node consists of 4 quaternionic degrees of freedom and there are $\chi = 2g - 2 + n$ thereof; generically on \mathcal{K} , the $SU(2)^{3g-3+n}$ gauge group breaks to $U(1)^g$, hence $3(3g - 3 + n) - g$ broken generators. Thus, there are effectively $4\chi - (3(3g - 3 + n) - g) = n + 1$ quaternionic degrees of freedom.

2.3 BPS Quivers

$\mathcal{N} = 2$ Gaiotto theories admit **BPS quivers** [9]. Let us briefly recall the details of these diagrams, following the discussion in [8]. We begin with a $(3 + 1)$ dimensional $\mathcal{N} = 2$ theory with Coulomb moduli space \mathcal{U} . At a generic point $u \in \mathcal{U}$, the theory has $U(1)^r$ gauge symmetry, and a low-energy solution defined by:

- A lattice Γ of electric, magnetic and flavour charges.
- An antisymmetric inner product on the charge lattice $\circ : \Gamma \times \Gamma \rightarrow \mathbb{C}$.
- A linear function $\mathcal{Z}_u : \Gamma \rightarrow \mathbb{C}$, the *central charge function* of the theory.

The central charge function \mathcal{Z}_u naturally appears in the $\mathcal{N} = 2$ algebra, and provides a lower bound on the masses of charged particles. The mass of a particle with $\gamma \in \Gamma$ satisfies $M \geq |\mathcal{Z}_u(\gamma)|$. The lightest charged particles are those that saturate this bound - these are termed **BPS states**.

The BPS quiver allows computation of the full BPS spectrum of the theory at some fixed point u in the Coulomb branch, supposing that the occupancy of the BPS states at that point is known [7]. This dramatically simplifies the problem of finding BPS states, since in place of some tedious weak coupling physics or prohibitively difficult strong coupling dynamics, the BPS spectrum is governed by a quantum mechanics problem encoded in the BPS quiver [7].

To construct a BPS quiver, first choose a half-plane \mathcal{H} in the complex \mathcal{Z}_u plane. All states with central charge in \mathcal{H} will be considered particles, while the states in the opposite half-plane will be considered anti-particles. Suppose there exists a set of hypermultiplet states $\{\gamma_i\}$ in the chosen half-plane that forms a positive integral basis for all particles. Given this basis $\{\gamma_i\}$, we can construct a BPS quiver as follows: For every charge γ_i , draw a node associated to it. For every pair of charges γ_i, γ_j with $\gamma_i \circ \gamma_j > 0$, draw $\gamma_i \circ \gamma_j$ arrows from γ_i to γ_j . The importance of the BPS quiver is that it can be used to check whether a particular site of the charge lattice $\gamma = \sum_i n_i \gamma_i \in \Gamma$ is occupied by a BPS state, and if so, to determine the spin and degeneracy of the associated particles. If we do this for every γ , we will have computed the full BPS spectrum of the theory at $u \in \mathcal{U}$ (for the details here, the reader is referred to [7, 8]).

Importantly, \mathcal{Z}_u varies from point to point in \mathcal{U} , hence its subscript u . A consequence of this is that the above procedure can yield different BPS quivers at different points $u \in \mathcal{U}$, thereby partitioning \mathcal{U} into domains, each corresponding to a different BPS quiver for the theory. For an $\mathcal{N} = 2$ Gaiotto theory, there is always a finite number of such BPS quivers [9]. Together, they are said to form a *finite mutation class*, and there

exists an algorithm, known as the *mutation method*, to enumerate all BPS quivers in a mutation class, once one has been specified.

Roughly, the principle on which the mutation method is based is as follows. Up to this point, we have arbitrarily chosen a half-plane \mathcal{H} in the complex \mathcal{Z}_u plane when constructing the BPS quiver. This choice of half-plane yields a unique basis of BPS states $\{\gamma_i\}$ and corresponding BPS quiver. Now consider rotating the half-plane clockwise by an angle θ , so that $\mathcal{H} \rightarrow \mathcal{H}_\theta = e^{-i\theta}\mathcal{H}$. As we tune θ from zero, nothing happens while all the $\{\gamma_i\}$ remain in the half-plane \mathcal{H}_θ . However, for some value of θ , the left-most state γ_1 will exit \mathcal{H}_θ on the left, while simultaneously the antiparticle state $-\gamma_1$ will enter on the right. Thus we will have a new basis of elementary BPS states $\{\tilde{\gamma}_i\}$ and a corresponding new BPS quiver. There is a simple algorithm for constructing this new basis of BPS states and corresponding BPS quiver from the old [7–9]. One full rotation of the half plane will enumerate the full mutation class of BPS quivers for the theory. It is important to remember that all the BPS quivers in a mutation class for a specific Gaiotto theory encode exactly the same physics [7–9].

2.4 Quadratic Differentials and Graphs on Gaiotto Curves

A **quadratic differential** on a Riemann surface S is a map

$$\phi : TS \rightarrow \mathbb{C} \tag{2.2}$$

satisfying $\phi(\lambda v) = \lambda^2 \phi(v)$ for all $v \in TS$ and all $\lambda \in \mathbb{C}$. If $z : U \rightarrow \mathbb{C}$ is a chart defined on some open set $U \subset S$, then ϕ is equal on U to

$$\phi_U(z) dz^2 \tag{2.3}$$

for some function ϕ_U defined on $z(U)$. Now suppose that two charts $z : U \rightarrow \mathbb{C}$ and $w : V \rightarrow \mathbb{C}$ on S overlap, with transition function $h := w \circ z^{-1}$; then if ϕ is represented

both as $\phi_U(z) dz^2$ and $\phi_V(w) dw^2$ on $U \cap V$, we have [16]

$$\phi_V(h(z)) (h'(z))^2 = \phi_U(z). \quad (2.4)$$

With these basic facts in mind, let us return to the $SU(2)$ Gaiotto theories of interest. Here, the Seiberg-Witten curves for these theories have the form $y^2 = \phi(x)$, where $q = \phi(x) dx^2$ is a quadratic differential on \mathcal{C} with only second order poles [5, 7]. (A subtlety: double poles in the quadratic differential only emerge for a mass-deformed theory. For vanishing mass deformation, the poles of the differential are single poles.) The functional form of q is specified by the topology $\langle g, n \rangle$ of the skeleton (we shall elaborate the exact details of this specification in the following section), and varying individual parameters in q amounts to changing the point in the moduli space under consideration. Since the Gaiotto theory in question is specified by $\langle g, n \rangle$, the Coulomb branch for each theory is determined by these two parameters; for this reason, we shall sometimes write $\mathcal{U}_{g,n}$ for the Coulomb branch of the Gaiotto theory with $\langle g, n \rangle$. In addition, q depends on n further positive real parameters associated to the n punctures of \mathcal{C} (which correspond to masses, couplings and moduli not fixed by moving in the Coulomb branch); the details of this dependence shall again be spelt out in the following section. To completely fix q requires us to fix a point in $\mathcal{U}_{g,n} \times \mathbb{R}_+^n$.

As we shall demonstrate in §3, the BPS quiver for a specific $\mathcal{N} = 2$ theory at a point $u \in \mathcal{U}$ can be constructed from a specific quadratic differential q on \mathcal{C} [7], by using the quadratic differential to construct a graph on \mathcal{C} known as its **ideal triangulation**, which has marked points as nodes and zeroes as faces. There is also a translation between BPS quivers and skeleton diagrams, which we shall again elaborate in §3 of this paper.

2.5 Dessins d’Enfants and Belyi Maps

There is a connection between the quadratic differentials on \mathcal{C} and Grothendieck’s **dessins d’enfants** [17–20]. Such a dessin is an ordered pair $\langle X, \mathcal{D} \rangle$ where X is an oriented compact topological surface (here the Gaiotto curve \mathcal{C}) and $\mathcal{D} \subset X$ is a finite graph satisfying the following conditions [17]:

1. \mathcal{D} is connected.
2. \mathcal{D} is *bipartite*, i.e. consists of only black and white nodes, such that vertices connected by an edge have different colours.
3. $X \setminus \mathcal{D}$ is the union of finitely many topological discs, which we call the *faces* of \mathcal{D} .

As we shall show in §3, at certain points in the Coulomb branch (and fixing in addition parameters associated to masses and couplings of the global flavour symmetries) we can use the quadratic differential to construct a graph on \mathcal{C} known as a **ribbon graph** [12], with marked points as faces and zeroes as nodes. At these points in the moduli space, the quadratic differential satisfies the conditions to be a so-called **Strebel differential**. As we shall see, we can interpret the ribbon graphs (with edge lengths set to be equal – corresponding to a *specific* fixing of the parameters associated to the flavour symmetries) as *dessins* by inserting a coloured node into every edge and colouring every vertex white; doing so leads to a number of interesting mathematical ramifications which cement *dessins* as important objects of study in the context of these $\mathcal{N} = 2$ theories (all of which shall be discussed in depth in the following section). In addition, we note here that if all the nodes of one of the two possible colours have valency two, then the *dessin* in question is referred to as *clean* [17].

Now recall that there is a one-to-one correspondence between *dessins d'enfants* and **Belyi maps** [17, 21]. A Belyi map is a holomorphic map to \mathbb{P}^1 ramified at only $\{0, 1, \infty\}$, i.e. for which the only points \tilde{x} where $\frac{d}{dx}\beta(x)|_{\tilde{x}} = 0$ are such that $\beta(\tilde{x}) \in \{0, 1, \infty\}$. We can associate a Belyi map $\beta(x)$ to a *dessin* via its *ramification indices*: the order of vanishing of the Taylor series for $\beta(x)$ at \tilde{x} is the ramification index $r_{\beta(\tilde{x}) \in \{0, 1, \infty\}}(i)$ at that i th ramification point [2, 13]. To draw the *dessin* from the map, we mark one white node for the i th pre-image of 0, with $r_0(i)$ edges emanating therefrom; similarly, we mark one black node for the j th pre-image of 1, with $r_1(j)$ edges. We connect the nodes with the edges, joining only black with white, such that each face is a polygon with $2r_\infty(k)$ sides (see e.g. [13, 20]).

2.6 The Modular Group and Congruence Subgroups

Finally, we should very briefly recall some essential details regarding the modular group $\Gamma \equiv \Gamma(1) = \text{PSL}(2, \mathbb{Z}) = \text{SL}(2, \mathbb{Z}) / \{\pm I\}$. This is the group of linear fractional transformations $\mathbb{Z} \ni z \rightarrow \frac{az+b}{cz+d}$, with $a, b, c, d \in \mathbb{Z}$ and $ad - bc = 1$. It is generated by the transformations T and S defined by:

$$T(z) = z + 1 \quad , \quad S(z) = -1/z . \quad (2.5)$$

The presentation of Γ is $\langle S, T | S^2 = (ST)^3 = I \rangle$.

The most important subgroups of Γ are the so-called *congruence* subgroups, defined by having the the entries in the generating matrices S and T obeying some modular arithmetic. Some conjugacy classes of congruence subgroups of particular note are the following:

- Principal congruence subgroups:

$$\Gamma(m) := \{A \in \text{SL}(2; \mathbb{Z}) ; A \equiv \pm I \pmod{m}\} / \{\pm I\};$$

- Congruence subgroups of level m : subgroups of Γ containing $\Gamma(m)$ but not any $\Gamma(n)$ for $n < m$;
- Unipotent matrices:

$$\Gamma_1(m) := \left\{ A \in \text{SL}(2; \mathbb{Z}) ; A \equiv \pm \begin{pmatrix} 1 & b \\ 0 & 1 \end{pmatrix} \pmod{m} \right\} / \{\pm I\};$$

- Upper triangular matrices:

$$\Gamma_0(m) := \left\{ \begin{pmatrix} a & b \\ c & d \end{pmatrix} \in \Gamma ; c \equiv 0 \pmod{m} \right\} / \{\pm I\}.$$

In [2], our attention is drawn to the conjugacy classes of a particular family of subgroups of Γ : the so-called *genus zero, torsion-free* congruence subgroups. By *torsion-free* we mean that the subgroup contains no element of finite order other than the

identity. To explain *genus zero*, first recall that the modular group acts on the upper half-plane $\mathcal{H} := \{\tau \in \mathbb{C}, \text{Im}(\tau) > 0\}$ by linear fractional transformations $z \rightarrow \frac{az+b}{cz+d}$. \mathcal{H} gives rise to a compactification \mathcal{H}^* when adjoining *cusps*, which are points on $\mathbb{R} \cup \infty$ fixed under some parabolic element (i.e. an element $A \in \Gamma$ not equal to the identity and for which $\text{Tr}(A) = 2$). The quotient \mathcal{H}^*/Γ is a compact Riemann surface of genus 0, i.e. a sphere. It turns out that with the addition of appropriate cusp points, the extended upper half plane \mathcal{H}^* factored by various congruence subgroups will also be compact Riemann surfaces, possibly of higher genus. Such a Riemann surface, as a complex algebraic variety, is called a **modular curve**. The genus of a subgroup of the modular group is the genus of the modular curve produced in this way. The conjugacy classes of the genus zero torsion-free congruence subgroups of the modular group are very rare: there are only 33 of them, with index $I \in \{6, 12, 24, 36, 48, 60\}$. [22]

3 A Web of Correspondences

In this section, we elaborate the chain of connections between skeleton diagrams, BPS quivers, ideal triangulations, ribbon graphs, quadratic differentials and Seiberg-Witten curves for $SU(2)$ Gaiotto theories. In §3.1, we present the connection between the quadratic differential $q = \phi(x) dx^2$ and Seiberg-Witten curve $y^2 = \phi(x)$ for these theories [5]. In §3.2, we show how the quadratic differential on \mathcal{C} encodes the *special Lagrangian flow* on this Riemann surface. We then describe how the ideal triangulation on \mathcal{C} is obtained. In §3.3, we recall how to construct a BPS quiver from a certain ideal triangulation [7]. Next, in §3.4 we show how to translate between skeleton diagrams and BPS quivers. In §3.5, we show how the special Lagrangian flow on \mathcal{C} can be used, at certain special points in the Coulomb branch where the quadratic differential becomes Strebel, to construct a ribbon graph on \mathcal{C} , and from this describe in detail how *dessins d'enfants* arise in the context of these theories, and the important roles they play in their study.

3.1 Quadratic Differentials and Seiberg-Witten Curves

The physics of an $SU(2)$ Gaiotto theory is determined by a Riemann surface \mathcal{C} of genus g with n punctures, one at each marked point $p_i \in \mathcal{C}$ [5]. We select a particular meromorphic quadratic differential $q = \phi(x) dx^2$ on \mathcal{C} . Fixing the behaviour of q at the points p_i by admitting a pole of finite order amounts to imposing that near p_i :

$$q(x) \sim \frac{1}{x^{k_i+2}} dx^2 \quad (3.1)$$

The integer $k_i \geq 0$ associated to each puncture is invariant under changes of coordinates. For the $SU(2)$ Gaiotto theories in question, we always choose $k_i = 0$ [5, 7]. The Seiberg-Witten curve Σ of the theory is given by a double cover of \mathcal{C} , and we obtain the **Seiberg-Witten differential** λ as follows [7]:

$$\Sigma = \{(x, y) \mid y^2 = \phi(x)\}, \quad \lambda = y dx = \sqrt{q} \quad (3.2)$$

Note that by varying the quadratic differential we obtain a family of Seiberg-Witten curves, and in this way the Coulomb branch $\mathcal{U}_{g,n}$ of the theory is naturally identified with the space of quadratic differentials obeying the boundary conditions from equation (3.1), *up to* a dependence on n further positive real parameters associated to the n punctures of \mathcal{C} (these numbers will turn out to be related to masses, couplings and moduli of the global flavour symmetries of the theory, not fixed by moving in the Coulomb branch). Thus, to completely fix q , we must fix a point in $\mathcal{U}_{g,n} \times \mathbb{R}_+^n$ [7, 12].

3.2 Trajectories on Riemann Surfaces and Ideal Triangulations

Consider a Riemann surface \mathcal{C} with a meromorphic quadratic differential q . Locally, we can write $q = \phi(x) dx^2$ for the appropriate local coordinate x on \mathcal{C} . Using this quadratic differential, we can classify parametric curves $\gamma(t)$ on \mathcal{C} according to the sign of q . *Horizontal trajectories* are defined as those for which $\phi(\gamma(t)) \dot{\gamma}(t)^2 > 0$, while

vertical trajectories are defined as those for which $\phi(\gamma(t))\dot{\gamma}(t)^2 < 0$ [12, 16]. There are three cases of importance in the study of these trajectories: a generic point on \mathcal{C} , a zero of q on \mathcal{C} , and a pole of q on \mathcal{C} .

Let us first consider a generic point on \mathcal{C} . To begin, suppose that $q = dx^2$. Then the horizontal trajectories are given by the horizontal lines $\alpha(t) = t + ci$ and the vertical trajectories are given by the vertical lines $\beta(t) = it + c$ [16]. Now, if a quadratic differential $q = \phi(x) dx^2$ is holomorphic and non-zero at $x = x_0$, then on a neighbourhood of x_0 we can introduce the canonical coordinate $w(x) = \int_{x_0}^x \sqrt{\phi(x)} dx$. It follows from the transformation rule (2.4) that in terms of the canonical coordinate the quadratic differential is given by $q = dw^2$, so at a generic point on \mathcal{C} the horizontal and vertical trajectories are horizontal and vertical lines, as shown in Figure 3(a) [12].

The situation is different where q either vanishes or has a pole. Let us consider what the horizontal and vertical trajectories look like in the vicinity of such points, which without loss of generality we shall take to be at zero. First, suppose that q vanishes here, so that $q = x^m dx^2$. Then, with $t \in \mathbb{R}^+$, the horizontal trajectories are given by $(m + 2)$ half-rays that have $x = 0$ on the boundary [12]:

$$\alpha_k(t) = t \cdot \exp\left(\frac{2\pi ik}{m+2}\right), \quad k = 0, 1, \dots, m+1. \quad (3.3)$$

The vertical trajectories are given by another set of $(m + 2)$ half-rays that have $x = 0$ on the boundary [12]:

$$\beta_k(t) = t \cdot \exp\left(\frac{\pi i + 2\pi ik}{m+2}\right), \quad k = 0, 1, \dots, m+1. \quad (3.4)$$

Thus we see that in the neighbourhood of zero both types of trajectory look like rays emanating from zero at some discrete angles, as shown in Figure 3(b). For a so-called *simple zero*, we have $m = 1$, and these trajectories make angles of $2\pi/3$ with each other [7].

Now consider the case where q has a second order pole. We take $q = -x^{-2} dx^2$. Then,

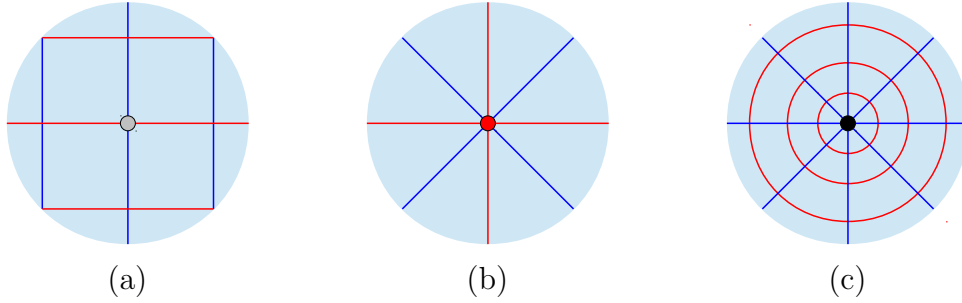


Figure 3: Horizontal (red) and vertical (blue) trajectories in the neighbourhood of (a) a generic point (marked in grey), (b) a zero of q (marked in red), and (c) a second order pole of q (marked in black) on \mathcal{C} .

horizontal trajectories are concentric circles centered at zero [12]:

$$\alpha(t) = r e^{it}, \quad t \in \mathbb{R}, \quad r > 0. \quad (3.5)$$

Vertical trajectories are given by half-rays emanating from zero [12]:

$$\beta(t) = t e^{i\theta}, \quad t > 0, \quad 0 \leq \theta < 2\pi. \quad (3.6)$$

These trajectories in the vicinity of a second order pole are hence as shown in Figure 3(c).

Note that we have only discussed second order poles. In [7], the analysis of the punctures is split into two cases depending on the order $k_i + 2$ of the pole in q . The *regular punctures* in \mathcal{C} are those for which $k_i = 0$. By Gaiotto's prescription, these are associated with flavour symmetries [5]. The *irregular punctures* in \mathcal{C} are those for which $k_i > 0$. For our purposes, we need consider only regular punctures: irregular punctures are associated with boundaries of \mathcal{C} , and none of the Gaiotto curves for the $SU(2)$ theories of interest have boundaries [5, 9].

The trajectories described define the *special Lagrangian flow lines* on \mathcal{C} [7]. Suppose that we have a surface \mathcal{C} with n marked points where q develops a second order pole. As we just saw, the horizontal trajectories are concentric rings around the marked points.



Figure 4: Ribbon graph (a) and corresponding ideal triangulation (b) for the $SU(2)$, $N_f = 4$ theory. Black nodes denote punctures of \mathcal{C} ; red nodes denote zeroes of q . The ideal triangulation has four faces, for the four zeroes of q .

This defines *domains* for each point. These domains are separated by the radial lines going between different zeroes of q . Only at very special points in the Coulomb branch $\mathcal{U}_{g,n}$ will these trajectories be such that they define a graph drawn on \mathcal{C} , where the marked points can be identified with the faces. Such a graph is known as a **ribbon graph** [12]; an extended discussion of such graphs and the circumstances in which they can be drawn is postponed to §3.5. It turns out that there are six topologically distinct possible ribbon graphs for a Gaiotto theory with one $SU(2)$ factor and $N_f = 4$ flavours; one example is drawn in Figure 4(a) (in this case, we know from [5] that the quadratic differential has the form $\phi = P_4(x)/\Delta_4^2(x)$, where P and Δ are polynomials in x and subscripts indicate polynomial degrees); the rest are drawn (as *dessins*) in Figure 6.

A convenient way to encode the topological structure of the special Lagrangian flow is in an **ideal triangulation** of \mathcal{C} . To construct such a triangulation, we consider one generic flow line which has its endpoints at two marked points on \mathcal{C} , and connect those two marked points by that trajectory. We repeat this for all pairs of marked points which are connected by such generic trajectories [7]. The structure of the flow on \mathcal{C} is such that each face of the resulting graph will have three edges and contain exactly one zero of q (in general we assume that these zeroes are simple, and thus have three radially outgoing trajectories, as discussed above) [7]. To illustrate, an ideal triangulation for a Gaiotto theory with one $SU(2)$ factor and $N_f = 4$ flavours is drawn in Figure 4(b).

In a sense, the ideal triangulation can be considered “dual” to the ribbon graph, as while an ideal triangulation has marked points as vertices and zeroes of the quadratic

differential as faces, the opposite is true for a ribbon graph. However, caution is needed here, as while it is generically true at *any* point in the Coulomb branch \mathcal{U} that one can construct an ideal triangulation on \mathcal{C} , one can *only* construct ribbon graphs, via the prescription involving horizontal and vertical trajectories above, at the *specific* points in \mathcal{U} (which will turn out to be the points where the quadratic differential on \mathcal{C} satisfies the stricter definition of being a *Strebel differential*, as discussed in section 3.5). The picture that emerges is therefore as follows. At any point in \mathcal{U} , one can construct an ideal triangulation. To each such ideal triangulation it is possible to associate a BPS quiver (see section 3.3). There are finitely many BPS quivers, so \mathcal{U} is partitioned into domains corresponding to each such BPS quiver. In addition, there are finitely many *specific points* in \mathcal{U} where one can construct a ribbon graph.

3.3 Constructing BPS Quivers

From the structure of an ideal triangulation on \mathcal{C} , there is a simple algorithm to extract the corresponding BPS quiver. We refer to an edge in the triangulation as a *diagonal* δ if the edge does not lie on a boundary of \mathcal{C} . (For the $SU(2)$ Gaiotto theories under consideration this makes no difference, since all the Gaiotto curves in this case are without boundary, as discussed.) The algorithm to construct a theory's BPS quiver from its ideal triangulation on \mathcal{C} is then as follows [7]:

- For each diagonal δ in the triangulation, draw one node of the BPS quiver.
- For each pair of diagonals δ_1 and δ_2 in the triangulation, find all the triangles for which both specified diagonals are edges. For each such triangle, draw one arrow connecting the nodes defined by δ_1 and δ_2 . Determine the direction of the arrow by looking at the triangle shared by δ_1 and δ_2 . If δ_1 immediately precedes δ_2 going anti-clockwise around the triangle, the arrow points from δ_1 to δ_2 .

For the derivation of this algorithm, the reader is referred to the original source [7]. It is straightforward to confirm that the BPS quiver for the Gaiotto theory with one $SU(2)$ factor and $N_f = 4$ flavours shown in Figure 1(b) can be constructed from the corresponding triangulation shown in Figure 4(b).

3.4 Skeleton Diagrams and BPS Quivers

With these connections between BPS quivers, ideal triangulations, flow diagrams, quadratic differentials on \mathcal{C} , and Seiberg-Witten curves established (following the details given in [7–9]), it remains to see how the skeleton diagrams for the corresponding $SU(2)$ Gaiotto theories enter the picture. To do this, first recall that each puncture of \mathcal{C} corresponds to a global $SU(2)$ flavour symmetry. Any two Gaiotto curves can be glued together by opening a hole at a puncture and gluing the two together with a tube; this results in gauging the $SU(2)$ groups corresponding to the two punctures [8]. By following this procedure, any Gaiotto curve can be constructed by gluing together three-punctured spheres; at the level of the skeleton, this simply amounts to joining trivalent vertices [3].

In [8] it is shown that this gluing procedure for the Gaiotto curves/skeleton diagrams can be translated into a gauging rule for the BPS quivers. To gauge a symmetry, we add gauge degrees of freedom and couple them to the matter already present in the theory. At the level of the quiver, this amounts to adding two nodes of a pure $SU(2)$ subquiver to add the gauge degrees of freedom, then coupling the existing pairs of identical nodes corresponding to the $SU(2)$ flavour symmetries to this subquiver. To do this, we delete one of the two identical nodes in each case and connect the other to the $SU(2)$ subquiver in an oriented triangle; the deleted state will then be generated by a bound state within the $SU(2)$ nodes [8].

Suppose that we are now given the skeleton diagram for the four-punctured sphere, as shown in Figure 1(a). This is the most basic legitimate skeleton diagram (one internal edge corresponding to one $SU(2)$ factor, formed by joining two trivalent vertices together); the corresponding BPS quiver was found in [7, 9], and is drawn in Figure 1(b). One can now construct any other legitimate skeleton diagram by appending more trivalent vertices onto any of the external legs; using the above procedure, one can construct a corresponding BPS quiver in every case. In this way, we obtain a precise translation between skeleton diagrams and BPS quivers for the $SU(2)$ Gaiotto theory in question, completing the backbone of correspondences in Figure 2. Once we have obtained one such BPS quiver, the rest in its finite mutation class can be computed using the mutation method [7–9]. An example of this gauging procedure for the case of gauging two

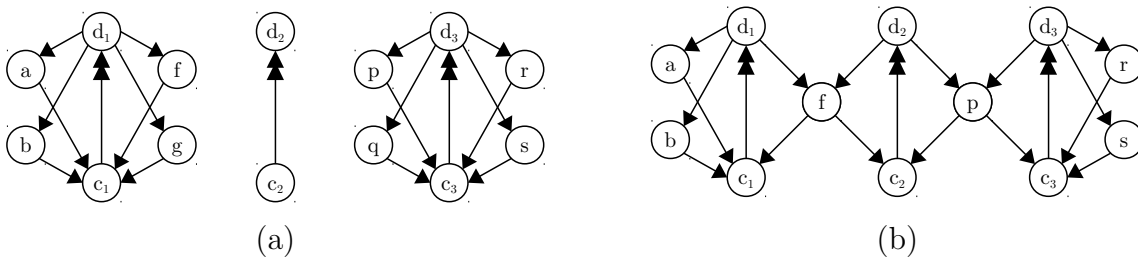


Figure 5: (a): The BPS quiver gauging procedure for joining the Gaiotto curves for two $SU(2)$ Gaiotto theories with $N_f = 4$. On the right and left we have the BPS quivers for these Gaiotto theories. In the centre we have introduced a pure $SU(2)$ subquiver to add the gauge degrees of freedom. (b): The resulting BPS quiver. The corresponding Gaiotto curve is a sphere with six punctures; this corresponds to an $SU(2)^3$ theory with $N_f = 6$. This is constructed from the components in (a) by deleting the nodes g and q and coupling f and p to the $SU(2)$ subquiver in oriented triangles.

$SU(2)$, $N_f = 4$ Gaiotto theories is provided in Figure 5.

From this, one might be tempted to conclude that all $SU(2)$ Gaiotto theories are susceptible to such a translation between their skeleton diagrams and BPS quivers. However, there are exceptions, specifically for the case of $SU(2)$ theories with $g > 2$ and $n = 0$. Such theories admit no mass deformations (for $g < 2$, one can see from the gluing procedure for skeleton diagrams that we must always have at least one external leg, and thus must have mass deformations), and hence do not admit BPS quivers [8, 9] - a point to which we shall return shortly in a different context. The case of $g = 2$ with no punctures is an exception: in one duality frame, that theory corresponds to an $SU(2)^3$ theory with two half-hypermultiplets; these two half-hypermultiplets form one full hypermultiplet and that can receive mass [9].

Using these results, we can now write down a skeleton diagram (all of which can be constructed by joining trivalent vertices) and immediately compute a wealth of information about the associated $SU(2)$ Gaiotto theory: the mutation class of BPS quivers, the BPS spectrum, the ideal triangulations on the Gaiotto curve \mathcal{C} corresponding to each BPS quiver, and the associated quadratic differentials on \mathcal{C} and Seiberg-Witten curves.

3.5 Strebel Differentials and Ribbon Graphs

3.5.1 Ribbon Graphs from Strebel Differentials

At a special point in the Coulomb branch $\mathcal{U}_{g,n}$ of the $SU(2)$ Gaiotto theory in question, the coefficients of the quadratic differential will be such that it satisfies the definition of a so-called **Strebel differential**. Choose an ordered n -tuple $(a_1, \dots, a_n) \in \mathbb{R}_+^n$ of positive real numbers. Then, a Strebel differential is a meromorphic quadratic differential q on a Riemann surface \mathcal{C} of genus g with n marked points $\{p_1, \dots, p_n\}$ (subject to the conditions $g \geq 0$, $n \geq 1$, and $2 - 2g - n < 0$) satisfying [12]:

1. q is holomorphic on $\mathcal{C} \setminus \{p_1, \dots, p_n\}$.
2. q has a second order pole at each p_j , $j = 1, \dots, n$.
3. The union of all non-compact horizontal trajectories forms a closed subset of \mathcal{C} of measure zero.
4. Every compact horizontal trajectory α is a simple loop circling around one of the poles, say p_j , satisfying $a_j = \oint_{\alpha} \sqrt{q}$, where the branch of the square root is chosen so that the integral has a positive value with respect to the positive orientation of α that is determined by the complex structure of \mathcal{C} .

Strebel differentials arise at specific points in $\mathcal{U}_{g,n}$. However, even at such points, the a_i are unfixed; such numbers are naturally associated with the residues of the n poles (physically, they can be associated with masses, couplings and moduli of the global flavour symmetries of the theory). Thus, to *completely* fix a Strebel differential, we must fix a point in $\mathcal{U}_{g,n} \times \mathbb{R}_+^n$. Note that the condition $n \geq 1$ ensures that no Strebel differential can be defined on $g \geq 2$, $n = 0$ Gaiotto curves. At the particular point in the Coulomb branch $\mathcal{U}_{g,n}$ of the theory where the quadratic differential is Strebel, the graph resulting from joining the zeroes of q via the horizontal trajectories, with one marked point for each face, is known as a **ribbon graph** [12].

3.5.2 Ribbon Graphs as Dessins

Now, it is at this point that Grothendieck's dessins d'enfants, i.e. bipartite graphs drawn on Riemann surfaces, enter the story. First, fix the point $u \in \mathcal{U}_{g,n}$ to be a point where the quadratic differential becomes Strebel. At such a point, one can construct a ribbon graph on \mathcal{C} . Then, fix the a_i to be such that the *lengths* of the edges of the ribbon graph are all equal. To do this, recall from [12] that the lengths $L(E_i)$ of the m edges of a ribbon graph enclosing its k th marked point are related to the associated number a_k by $a_k = \sum_{i=1}^m L(E_i)$; writing down such an equation for all marked points, one can solve the system of simultaneous equations to determine the lengths of the edges of the ribbon graph. By convention, choose all these lengths to equal unity.

As discussed in [12], at such a point in $\mathcal{U}_{g,n} \times \mathbb{R}_+^n$, the ribbon graph on \mathcal{C} for each Gaiotto theory can be interpreted as a clean dessin d'enfant, by colouring every vertex white and inserting a black node into every edge. In turn, we can associate a unique Belyi map to every such dessin by following the procedure detailed in §2.5. The Belyi map $\beta(x)$ determined by the ribbon graph in this way then possesses an interesting property [12]: the Strebel differential $\phi(x) dx^2$ on \mathcal{C} , fixing the a_i so that all ribbon graph edges are equal to unity, can be constructed as the pullback by $\beta(x)$ of a quadratic differential on \mathbb{P}^1 with coordinates ζ with three punctures:

$$q = \phi(x) dx^2 = \beta^* \left(\frac{1}{4\pi^2} \frac{d\zeta^2}{\zeta(1-\zeta)} \right). \quad (3.7)$$

In other words, the map $\beta(x)$ from \mathcal{C} to \mathbb{P}^1 is precisely the Belyi map corresponding to the ribbon graph interpreted as a dessin [12]. Clearly, it follows immediately from the definition of the pullback that we can write:

$$q = \frac{1}{4\pi^2} \frac{d\beta^2}{\beta(1-\beta)}. \quad (3.8)$$

In itself, this is an extremely intriguing result. However, we can go further, by now recalling **Belyi's theorem**. This states that a non-singular Riemann surface \mathcal{C} has the

structure of an algebraic curve defined on $\overline{\mathbb{Q}}$ if and only if there is a Belyi map from \mathcal{C} onto \mathbb{P}^1 [12, 17]. By this theorem, our Gaiotto curves (save the exceptional $g \geq 2$, $n = 0$ cases discussed, where we cannot draw a ribbon graph on \mathcal{C}) have the structure of algebraic curves defined on $\overline{\mathbb{Q}}$, at these particular points in $\mathcal{U}_{g,n} \times \mathbb{R}_+^n$.

3.5.3 Strebel Differentials from Belyi Maps

Suppose we are given one possible ribbon graph on \mathcal{C} . With this in hand, (3.8) provides a means of directly computing the associated Strebel differential (for the point in \mathbb{R}_+^n where all edges are equal): we simply substitute the associated Belyi map into this formula. For example, consider the ribbon graph given in figure 4(a), for the $SU(2)$, $N_f = 4$ theory. The Belyi map associated to this tetrahedral ribbon graph, as a dessin, is given in [23]:

$$\beta_{\text{tetra}}(z) = -64 \frac{z^3(z^3 - 1)^3}{(1 + 8z^3)^3}. \quad (3.9)$$

The pre-images of $\{0, 1, \infty\}$ for this Belyi map are, respectively, $\{3^4, 2^6, 3^4\}$ [13]. Substituting $\beta_{\text{tetra}}(z)$ into (3.8) gives:

$$q = -\frac{576z(z^3 - 1)}{4\pi^2(1 + 8z^3)^2}. \quad (3.10)$$

This quadratic differential has poles at $\left\{-\frac{1}{2}, \frac{1}{2}(-1)^{1/3}, -\frac{1}{2}(-1)^{2/3}, \infty\right\}$. This is the Strebel differential on \mathcal{C} associated to the tetrahedral ribbon graph (with equal length edges) for the $SU(2)$, $N_f = 4$ Gaiotto theory. Note that this correctly matches the generic expected form of the quadratic differential for the $SU(2)$, $N_f = 4$ theory, as presented in [5, 26] and discussed in the following section of this paper. Clearly, the above method provides an efficient means of computing explicit Strebel differentials on \mathcal{C} .

3.5.4 Enumerating Ribbon Graphs

At this point, a further question naturally arises: for a given $SU(2)$ Gaiotto theory, how do we enumerate all topologically distinct possible ribbon graphs? In order to answer this question, we first need to know, for a given $SU(2)$ Gaiotto theory, the most general possible form of the quadratic differential on \mathcal{C} . This can be computed in the following way. First, suppose we have a Gaiotto theory with n punctures on \mathcal{C} , so that the associated ribbon graphs have n faces. Given this, the number of *vertices* of the ribbon graphs can be computed using Euler's formula, which relates the number of vertices V , edges E and faces F of a graph drawn on a surface of genus g :

$$V - E + F = 2 - 2g. \tag{3.11}$$

Since we assume all our ribbon graphs have simple zeroes and are thus trivalent and connected, we have $E = \frac{3}{2}V$. From the above reasoning, $F = n$. Thus:

$$V = 2n - 4 + 4g. \tag{3.12}$$

Thus we can construct the quadratic differential for the theory in question given only the topology $\langle g, n \rangle$ of the skeleton: generically, this will have n second-order poles and $2n - 4 + 4g$ faces. Note, however, that we can *only* apply this method for the class of $SU(2)$ Gaiotto theories which admit such a differential; for $g \geq 2$, $n = 0$, this is not possible, since in this case one cannot construct a quadratic differential on \mathcal{C} with only second order poles [12], as we have already observed. Setting aside the exceptional case of $g = 2$, $n = 0$ already discussed, this result is reassuring. This is because we have already found that for $g \geq 2$, $n = 0$, the theory in question does not admit a BPS quiver. But since we can translate between the quadratic differential and the BPS quiver as described, we would expect to find that in these cases we cannot write down a quadratic differential of the generic form described above. Indeed we now see this to be the case.

So, the generic form of a ribbon graph on \mathcal{C} will have n faces (corresponding to second-

Number of faces (n)	Number of vertices ($2n - 4$)	Index of dessin	Gaiotto theory
4	4	12	$SU(2)$, $N_f = 4$
6	8	24	$SU(2)^3$, $N_f = 6$
8	12	36	$SU(2)^5$, $N_f = 8$
10	16	48	$SU(2)^7$, $N_f = 10$
12	20	60	$SU(2)^9$, $N_f = 12$

Table 1: The number of faces and vertices of a ribbon graph drawn on a genus zero Gaiotto curve, as well as the index of the dessins from [13] which match those numbers of faces and vertices.

order poles of q), and $2n - 4 + 4g$ vertices (corresponding to zeroes of q). Any ribbon graph which fulfils these topological criteria is a possible ribbon graph for the Gaiotto theory in question, and its associated Strebel differential, for the case of equal length edges, can be computed via the ribbon graph's corresponding Belyi map in the manner detailed above. For details on algorithmic procedures for enumerating all possible trivalent graphs with a given number of vertices and edges, the reader is referred to the classic works [27–29], as well as the discussion in [2].

3.5.5 Connections to Modularity

It is interesting to note that the six topologically distinct possible ribbon graphs for the $SU(2)$, $N_f = 4$ theory correspond to the dessins for the index 12 modular subgroups presented in [2, 13, 22]. For ease of reference, these are presented in Figure 6. With this in mind, the question arises as to which $SU(2)$ Gaiotto theories the remaining dessins in [13] correspond, insofar as they are possible ribbon graphs on \mathcal{C} . To answer this question, first recall that all the dessins in question are drawn on the sphere, so we must have $g = 0$. In addition, each dessin must have n faces, where n is the number of punctures on \mathcal{C} for the theory in question. From the work in the previous section, the dessin must therefore have $V = 2n - 4$ vertices.

The number of faces and vertices for important values of n are tabulated in Table 1. The reader can note that the number of faces and vertices of a ribbon graph drawn on a genus zero Gaiotto curve precisely match those of the various index dessins in [13],

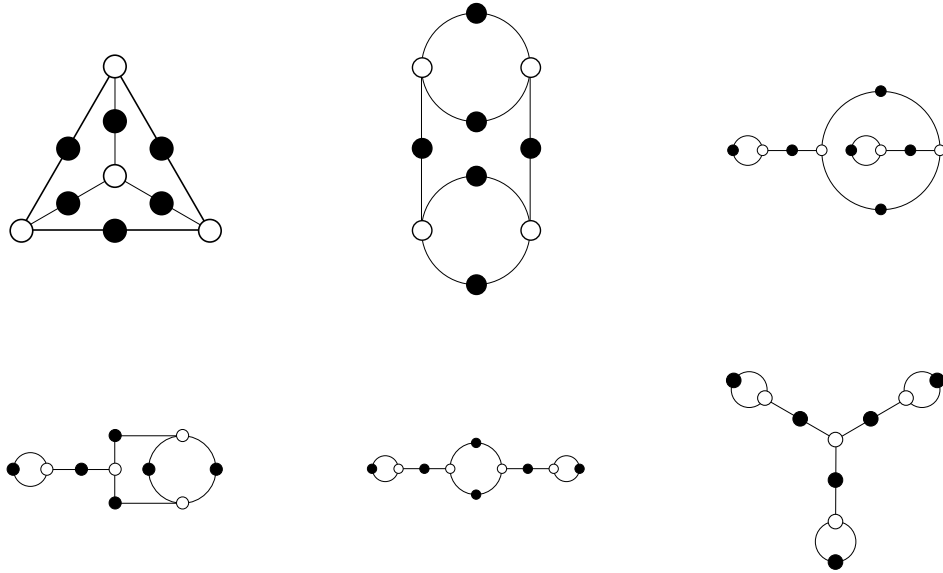


Figure 6: The six possible ribbon graph topologies for the $SU(2)$, $N_f = 4$ theory, drawn as dessins d'enfants. These are precisely the six index 12 dessins in [13].

as given in the third column of Table 1. Hence, one can see that the dessins in [13] do correspond to ribbon graphs of certain Gaiotto theories.

Which Gaiotto theories are these? Since the skeleton diagrams for an $SU(2)$ Gaiotto theory can all be constructed by joining trivalent vertices, for a genus zero Gaiotto curve, we simply need to join repeated trivalent vertices, without loops, until the right number of punctures is reached. (Recall that each internal leg of a skeleton diagram corresponds to an $SU(2)$ gauge group factor; each external leg corresponds to a puncture, and thereby to an external flavour symmetry.) The resulting skeleton diagram with n external legs gives the Gaiotto theory to which the dessin in question – with n vertices and $2n - 4$ faces – corresponds. The results of undertaking this process are given in the fourth and final column of Table 1.

3.5.6 Location of the Strebel Points in the Coulomb Branch

What, then, is the physical significance of these ribbon graphs, which arise where the quadratic differential on \mathcal{C} satisfies the definition of a Strebel differential? As stated in §6 of [6], flow lines form closed orbits around marked points precisely where a BPS state appears and the topology of the triangulation (and thus BPS quiver) jumps. Hence, if the Coulomb branch is partitioned into domains for each BPS quiver of the theory, these Strebel points in the moduli space must arise at the walls *separating* these domains.

3.5.7 Dessins at Other Points in the Moduli Space

It is worth making a further comment on the form (3.8) of the quadratic differential q in terms of a Belyi map β . Though at a Strebel point q can be written in this form, with the Belyi map then being that associated to the ribbon graph (with equal length edges) interpreted as a dessin, this does not preclude us from being able to write q in the form (3.8) at some *other* isolated points in the moduli space.¹ The reason for this is that Theorem 6.5 of [12] is an ‘if’ rather than an ‘if and only if’ statement in this respect. Indeed, we can find such a point in the moduli space as in the following example. Consider again the $SU(2)$, $N_f = 4$ theory, but this time begin with the generic form of the quadratic differential, with four simple zeroes and four second-order poles. We parameterise this generic form as

$$\phi(x) = \frac{(u_1x^2 + m_1x + l_1)^2 - 4(u_0x^2 + m_0x + l_0)(u_2x^2 + m_2x + l_2)}{4x^2(u_2x^2 + m_2x + l_2)^2}, \quad (3.13)$$

with $q = \phi(x) dx^2$. Now, choosing

$$u_2 = -(4 + 3\sqrt{2})\pi \quad u_1 = i(4 + 3\sqrt{2}) - \frac{\sqrt{2}}{3}m_1 \quad u_0 = \frac{6i\sqrt{2} + (4 - 3\sqrt{2})m_1}{36\pi}m_1$$

¹We thank Diego Rodriguez-Gomez for pointing out this possibility, and for the calculations which follow in this subsection.

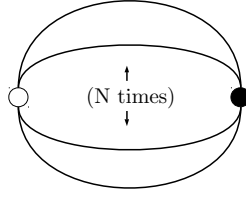


Figure 7: Dessin for the Belyi map $\beta_N(x)$. For $N = 4$, we have a 4-valent white node joined to a 4-valent black node on \mathbb{P}^1 .

$$\begin{aligned}
 l_2 &= -\left(4 + 3\sqrt{2}\right) \pi & l_1 &= \frac{3i\sqrt{2} + (3\sqrt{2} - 4)}{6\sqrt{2} - 9} m_1 & l_0 &= -\frac{6i\sqrt{2} + (3\sqrt{2} - 4)}{36\pi} m_1 \\
 m_2 &= 3\left(3 + 2\sqrt{2}\right) \pi & m_0 &= \frac{36 + 24\sqrt{2} + (3 - 2\sqrt{2}) m_1^2}{12\pi}
 \end{aligned} \tag{3.14}$$

we have, upon doing the transformation

$$x \rightarrow \frac{x - \frac{1}{2} \left(1 - i\sqrt{3 - 2\sqrt{2}}\right)}{x - \frac{1}{2} \left(1 + i\sqrt{3 - 2\sqrt{2}}\right)} \tag{3.15}$$

a differential in our “canonical” Strebel form (3.8), this time with Belyi map

$$\beta(x) = \frac{x^4}{x^4 + (x - 1)^4}. \tag{3.16}$$

What is the dessin corresponding to this Belyi map? In fact, it is known from [23, 30] that a Belyi map of the form

$$\beta_N(x) = \frac{x^N}{x^N + (x - 1)^N} \tag{3.17}$$

has an associated dessin of the form shown in Figure (8).

The first thing to notice about this dessin is that it is *not* clean. But since all the dessins associated to ribbon graphs are by construction clean, this means that this dessin cannot correspond to a ribbon graph. In turn, this means that this specific point in the moduli space cannot be Strebel – i.e. q is not a Strebel differential at this point. Hence we see that, starting from the generic expression for the quadratic differential for a certain theory and tuning parameters in the way describe above, one does not *necessarily* arrive at a form (3.8) which corresponds to a Strebel point (note, though, that all the Strebel points can be found simply by fixing parameters in q , whereas in the above we also needed to transform x).

Whether these non-Strebel dessins have any significance is an open question. One must approach such results with a certain degree of caution, since it is not clear what significance the form of the quadratic differential (3.8) has away from the Strebel points. Nevertheless, these auxiliary dessins which arise at other points in the moduli space in this way present an interesting opportunity for future investigation.

3.5.8 Further Conjectures

Based on the above work, one might attempt to link previous work on the connections between dessins d’enfants and $\mathcal{N} = 2 U(N)$ gauge theories presented in [10, 11] to the $SU(2)$ Gaiotto case. In this section we will see, however, that the analogy is at least not a direct one, and several aspects of it fail.

To begin, first recall that in [10] the authors demonstrate how the problem of finding Argyres-Douglas singularities in the Coulomb branch \mathcal{U} of an $\mathcal{N} = 2$ theory with $U(N)$ gauge group can be mapped to the problem of finding when an abstractly defined quadratic differential on a Riemann surface becomes Strebel. Moreover, at these special Argyres-Douglas points, the Belyi map associated to the ribbon graph (interpreted as a dessin) for that Strebel differential can be used to construct the Seiberg-Witten curve of the theory. This is a purely formal correspondence, but the work above suggests that these quadratic differentials and dessins have a nice interpretation for $SU(2)$ Gaiotto theories: the quadratic differentials are precisely the quadratic differentials on the Gaiotto curves which appear in the Seiberg-Witten curves, while the dessins d’enfants

are precisely the ribbon graphs drawn on the Gaiotto curves.

Is this conjecture correct? To evaluate it, we must recall some further details from [10]. In that paper, the authors consider the ribbon graph associated to the abstractly defined quadratic differentials. If we take such a ribbon graph and interpret as a dessin, we can find the associated Belyi map, which can generically be expressed as

$$\beta(z) = \frac{A(z)}{B(z)}, \quad (3.18)$$

where $A(z)$ and $B(z)$ are polynomials of some degree. In turn, this Belyi map can be used to construct the Seiberg-Witten curve for the $U(N)$ gauge theory in question via the identification

$$y^2 = P^2(z) + B(z), \quad (3.19)$$

where

$$P^2(z) = A(z) - B(z). \quad (3.20)$$

Given this identification of the polynomials of the Belyi map with the right hand side of the Seiberg-Witten curve in hyperelliptic form, it is clear that if the quadratic differential discussed in [10] can indeed be interpreted as the quadric differential on the Gaiotto curve in the case of $SU(2)$ Gaiotto theories, it must be the case that at the points in the moduli space of the theory where this becomes Strebel, the associated Belyi map yields a Seiberg-Witten curve in hyperelliptic form of the correct degree for the theory in question. This is a proposition which can be easily tested in a concrete example; we will choose for simplicity the $SU(2)$, $N_f = 4$ theory.

The Belyi map for the tetrahedral ribbon graph for this theory is given in (3.10). From this, we can see that the numerator is a degree 9 polynomial in z . Hence, on the above prescription, the Seiberg-Witten curve for this theory has the form $y^2 = A_9(z)$.

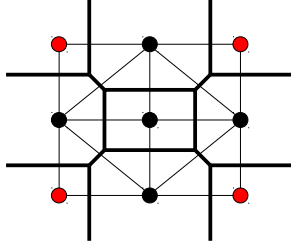


Figure 8: Braneweb and grid diagrams for the $SU(2)$, $N_f = 4$ theory.

However, the Seiberg-Witten curve for this theory is in fact of degree *four*. We can reason to this answer in the following way.

First, this theory can be seen as the dimensional reduction of the five dimensional theory living on the braneweb shown in Figure 8. The Seiberg-Witten curve corresponding to the 5D theory living on the sphere is [31]

$$\tilde{L}_2 + \tilde{y}\tilde{M}_2 + \tilde{y}^2\tilde{U}_2 = 0, \quad (3.21)$$

where \tilde{L}_2 , \tilde{M}_2 and \tilde{U}_2 are degree two polynomials in \tilde{x} whose coefficients are associated to the dots in the grid diagram. In this curve, the holomorphic two-form is $d\lambda = d\log x \wedge d\log y$. The standard reduction to 4D amounts to taking $\tilde{y} = y$ and $\tilde{x} = e^{2\epsilon x}$. In the appropriate $\epsilon \rightarrow 0$ limit [33, 34], the curve becomes

$$L_2 + yM_2 + y^2U_2 = 0, \quad (3.22)$$

with the expected holomorphic two-form $dx \wedge d\log y$. Note that the polynomials L_2 , M_2 and U_2 are not the same as \tilde{L}_2 , \tilde{M}_2 and \tilde{U}_2 . Indeed, the first terms in the ϵ expansion of the coefficients of the latter reshuffle in some way to construct the former. Now, upon doing

$$y = \frac{1}{U_2} \left(t - \frac{M_2}{2} \right), \quad (3.23)$$

we find:

$$t^2 = \frac{M_2^2}{4} - L_2 U_2. \quad (3.24)$$

Clearly, the hyperelliptic curve for this theory is degree four in the right hand side, not degree nine. The upshot of this is that we cannot use the Belyi map associated to a given Strebel differential on \mathcal{C} to construct the appropriate Seiberg-Witten curve, as for the abstractly defined quadratic differentials in [10, 11]. Of course, it is still possible that the points in the Coulomb branch at which the quadratic differential on \mathcal{C} becomes Strebel give interesting factorisations of the Seiberg-Witten curves as in [10, 11], but more work needs to be done to establish this point. At the very least, the connections to the work of the cited papers is not as straightforward as one might hope.

3.6 Taking Stock

Let us briefly recap the results gathered up to this point. Take a Gaiotto curve \mathcal{C} of genus g with n punctures. The Seiberg-Witten curve for this theory has the form $y^2 = \phi(x)$, where $q = \phi(x) dx^2$ is a meromorphic quadratic differential on \mathcal{C} . The precise number of zeroes and second-order poles which this quadratic differential possesses was computed in §3.5.4. From the quadratic differential one can construct an ideal triangulation, and in turn the mutation class of BPS quivers for the theory in question, as detailed in §3.2-3.4.

The parameters of the quadratic differential vary as one varies the point in the Coulomb branch $\mathcal{U}_{g,n}$ under consideration. At certain very special points, q will satisfy the definition of a Strebel differential; at these points we can draw a ribbon graph on \mathcal{C} . To completely fix q , we must fix n further positive real parameters, associated to the lengths of the edges of the ribbon graph. Fixing these parameters such that the edge lengths are unity (and thus completely fixing q by fixing a point in $\mathcal{U}_{g,n} \times \mathbb{R}_+^n$), this ribbon graph can be interpreted as a trivalent dessin d'enfant, with an associated Belyi map. The Belyi map relates q at this point to a meromorphic quadratic differential on \mathbb{P}^1 by pullback, as detailed in §3.5.1-3.5.2. In this way, as detailed in §3.5.3, we can reconstruct

Strebel differentials at such points just given possible ribbon graph topologies on \mathcal{C} .

In §3.5.5, we identified the Gaiotto theories to which the dessins in [13] correspond, insofar as they are possible ribbon graphs for those theories; in §3.5.6 we identified the location of the Strebel points in the Coulomb branch of these theories. In §3.5.7 we investigated the possibility of the form (3.8) of the quadratic differential arising at non-Strebel points. Finally, in §3.5.8, we demonstrated that one cannot straightforwardly identify the quadratic differential on \mathcal{C} with the abstractly defined quadratic differentials in [10, 11], as doing so yields inconsistent results.

4 Skeleton Diagrams to Seiberg-Witten Curves: An Alternative Route?

In [2], it is stated that the skeleton diagrams should be interpreted *directly* as dessins d'enfants; from there it is claimed that we can construct the corresponding Seiberg-Witten curve by manipulating the Belyi map associated to this dessin. In this section we show that this deployment of dessins cannot work in general, as the method cannot guarantee that the Seiberg-Witten curve will have the correct form. To do this, we follow the methodology of [2], where the authors consider the specific class of dessins corresponding to the 33 genus zero, torsion-free congruence subgroups of the modular group Γ (introduced in §2.6), all of which have $g > 0$ and $n = 0$, interpreting these as skeleton diagrams.

The general setup is as follows: we suppose that we have a skeleton diagram with g loops and n external legs, topologically identical to one of dessins in [2]. We interpret this as a dessin: exactly the corresponding dessin in [2]. We then attempt to follow the prescription in [2] to construct the Seiberg-Witten curve corresponding to the original skeleton diagram from the Belyi map for the associated dessin. We do this for a wide class of skeletons (all of which are topologically identical to dessins in [2]), showing that the proposed method fails for some of these skeleton diagrams. Therefore, the proposed route from skeleton diagrams to Seiberg-Witten curves needs to be modified, in the manner presented below.

With the above in mind, let us begin our investigations. First recall from [9] that the genus of the Seiberg-Witten curve $g(\Sigma)$ is related to the genus of the Gaiotto curve $g(\mathcal{C})$ by the following formula, where p_i denotes a puncture on \mathcal{C} , and we consider separately punctures of odd and even order:

$$g(\Sigma) = 4g(\mathcal{C}) - 3 + \frac{1}{2} \sum_{p_i \text{ even}} p_i + \frac{1}{2} \sum_{p_i \text{ odd}} (p_i + 1). \quad (4.1)$$

The genus of the Gaiotto curve $g(\mathcal{C})$ is determined by the number of loops of the skeleton diagram, so we find, by considering the number of loops of each of these dessins in [13], that for a skeleton diagram (interpreted as a dessin) corresponding to a genus zero, torsion-free, congruence subgroup of index I , the genus of the Gaiotto curve is given by

$$g(\mathcal{C}) = \frac{I}{6} + 1. \quad (4.2)$$

Thus we have from (4.2) and (4.3) (noting that in our case all p_i are even, since they are of order 2):

$$g(\Sigma) = \frac{2I}{3} + 1. \quad (4.3)$$

Now, any hyperelliptic curve has the equation $y^2 = Q_N(x)$, where $Q_N(x)$ is a degree N polynomial in x . A genus $g(\Sigma)$ hyperelliptic curve has the equation $y^2 = Q_{2g(\Sigma)+1}(x)$ (for an imaginary hyperelliptic curve) or $y^2 = Q_{2g(\Sigma)+2}(x)$ (for a real hyperelliptic curve). Using our above result for $g(\mathcal{C})$, we therefore find that the Seiberg-Witten curves corresponding to our index I dessins can be written in the form $y^2 = Q_{4I/3+3}(x)$ in the imaginary case, and $y^2 = Q_{4(I/3+1)}(x)$ in the real case. Thus the degrees of the polynomials in the Seiberg-Witten curves for the indices I of interest from [2] (i.e. $I \in \{6, 12, 24, 36, 48, 60\}$) are as shown in Table 2.

For a dessin corresponding to an index I subgroup, the corresponding Belyi map $\beta(x)$ is a quotient of two polynomials $A(x)$ and $B(x)$, the difference of which is equal

Index I	$\deg(Q_{4I/3+3}(x))$	$\deg(Q_{4(I/3+1)}(x))$
6	11	12
12	19	20
24	35	36
36	51	52
48	67	68
60	83	84

Table 2: The degrees of the Seiberg-Witten curves for an $\mathcal{N} = 2$ $SU(2)$ Gaiotto theory where the skeleton diagram is a dessin d'enfant corresponding to a genus zero, torsion-free, congruence subgroup of index I . The second column corresponds to the imaginary hyperelliptic case; the third to the real hyperelliptic case.

to the square of a polynomial of degree $I/2$ [2, 11]:

$$A(x) - B(x) = P_{I/2}^2(x). \quad (4.4)$$

It is at this point that the conjecture in this approach begins. We need some procedure taking us from $P_{I/2}(x)$ on the dessin side to $Q_{4(I/3+1)}(x)$ on the Seiberg-Witten side (focussing on the case of real hyperelliptic curves - the situation for imaginary hyperelliptic curves is analogous). As a matter of simply matching degrees, we have:

$$a \cdot \deg(P_{I/2}(x)) = \deg(Q_{4(I/3+1)}(x)). \quad (4.5)$$

Solving for a , we find:

$$a = 8 \left(\frac{1}{3} + \frac{1}{I} \right). \quad (4.6)$$

For the indices of interest in [2] ($I \in \{6, 12, 24, 36, 48, 60\}$), we have the results shown in Table 3.

The thought at this point is that we can then simply identify $P_{I/2}^a(x)$ from the Belyi

Index I	Exponent a in (4.6)
6	4
12	$10/3$
24	3
36	$26/9$
48	$17/6$
60	$14/5$

Table 3: The power a to which a polynomial of degree $I/2$ must be raised to produce a function (possibly polynomial) of degree $4(I/3 + 1)$. This procedure allows us to match the degree of $P_{I/2}(x)$ from the Belyi map corresponding to the skeleton diagram interpreted as a dessin d'enfant to the expected degree of the Seiberg-Witten curve for the Gaiotto theory in question.

map associated to the skeleton diagram interpreted as a dessin with $Q_{4(I/3+1)}(x)$: the Seiberg-Witten curve for that gauge theory in hyperelliptic form. Clearly, there is something special about index 6 and index 24, if this procedure for going from $P_{I/2}(x)$ to $Q_{4(I/3+1)}(x)$ is correct. This is because only index 6 and index 24 give integer a , and therefore guarantee polynomial Q , as required when constructing a Seiberg-Witten curve. *But for every $SU(2)$ gauge theory of Gaiotto type, there is a Seiberg-Witten curve which can be associated with the skeleton diagram.* Therefore, we see that, when dessins for which $I \notin \{6, 24\}$ are considered, the fact that this method cannot guarantee that $Q(x)$ is a polynomial demonstrates that it is in general *not correct*. Thus, in such cases, and hence in general, interpreting the skeleton diagram as a dessin d'enfant and attempting to construct the corresponding Seiberg-Witten curve from the Belyi map in this way will not work.

Indeed, there is no reason to suspect any direct connection between skeleton diagrams and Seiberg-Witten curves via the theory of dessins d'enfants (although, as, we have seen, dessins *do* arise in the context of the ribbon graphs). Moreover, this method clearly only works when we consider skeleton diagrams without external legs, since it is unclear what external legs of a dessin would mean. To conclude then: the correct method for matching the skeleton diagrams to the corresponding quadratic differentials and Seiberg-Witten curves is outlined in §2 and §3 of this paper; the work there supersedes the work presented in this section.

5 Conclusions and Outlook

In this paper, we have first recapitulated several significant results from [2,3,7–9] in order to present an explicit web of connections relating important mathematical structures in the study of $SU(2)$ Gaiotto theories. This is the backbone of connections in Figure 2. Undertaking this task has allowed us to pinpoint the precise manner in which dessins d’enfants arise in the context of these theories. Our conclusions are as follows:

- At a certain point in the Coulomb branch $\mathcal{U}_{g,n}$, the quadratic differential on \mathcal{C} for the Gaiotto theory in question is Strebel. At such a point, the horizontal trajectories join to form a graph on \mathcal{C} known as a *ribbon graph* [12]. When the edges of this ribbon graph are of equal length (found by fixing a particular point in $\mathcal{U}_{g,n} \times \mathbb{R}_+^n$), this graph can be interpreted as a clean dessin.
- The ribbon graph, interpreted as a dessin, has a unique corresponding Belyi map $\beta : \mathcal{C} \rightarrow \mathbb{P}^1$. This Belyi map relates the Strebel differential on \mathcal{C} at this point in $\mathcal{U}_{g,n} \times \mathbb{R}_+^n$ and a meromorphic quadratic differential on \mathbb{P}^1 by pullback.
- By Belyi’s theorem, the fact that this is possible for almost all Gaiotto theories means that almost all Gaiotto curves have the structure of algebraic curves defined over $\overline{\mathbb{Q}}$, at these particular points in $\mathcal{U}_{g,n} \times \mathbb{R}_+^n$.
- Consideration as to the topology of the ribbon graphs yields a means of computing the essential features of the quadratic differential in question: it must have n second order poles and $2n - 4 + 4g$ zeroes. Possible ribbon graph topologies for a Gaiotto theory with \mathcal{C} having n punctures and genus g therefore have n faces and $2n - 4 + 4g$ vertices.
- This yields an efficient means of computing the explicit Strebel differentials, and hence Seiberg-Witten curves, at these points in $\mathcal{U}_{g,n} \times \mathbb{R}_+^n$: for the $\langle g, n \rangle$ Gaiotto theory in question, we compute all possible trivalent connected graphs with n faces and $2n - 4 + 4g$ vertices, interpret as dessins, compute the associated Belyi maps, and substitute into (3.8).
- The dessins in [13] correspond to possible ribbon graphs of specific $SU(2)$ Gaiotto theories, which have been identified.

- Ribbon graphs appear at points in the Coulomb branch where the triangulation (and hence BPS quiver) jumps.
- In [10, 11], it was found that the problem of finding Argyres-Douglas singularities for $U(N)$ $\mathcal{N} = 2$ gauge theories can be mapped to the problem of finding points where an abstractly defined quadratic differential becomes Strebel; and therefore mapped to the problem of constructing dessins. We have found that there are difficulties in straightforwardly extending this story to the $SU(2)$ Gaiotto theories under consideration in this paper.

These conclusions establish the “lower loop” of connections in Figure 2, as well as fleshing out many more details. The means of immediately writing down the functional form of the quadratic differential q given topology $\langle g, n \rangle$ of the skeleton diagram is the “upper arc” of Figure 2. Moreover, we have shown in §4 that the method proposed in [2] for writing down the Seiberg-Witten curve for such a theory by interpreting the skeleton diagram as a dessin must be modified in general.

There are many possible extensions of this work. Most notably, it would be a valuable task to understand better the physical significance of the points in the moduli space where ribbon graphs can be constructed (i.e. the Strebel points), beyond the observation that these points lie on boundaries separating BPS domains of the Coulomb branch. Indeed, the authors are currently collaborating on a further paper investigating these Strebel points from the point of view of Liouville conformal field theories via the AGT conjecture [32]; the hope is that such investigations will shed further light on the significance of these points, and the dessins that arise in these $\mathcal{N} = 2$ theories.

In addition, it would be interesting to investigate whether the Seiberg-Witten curves for these theories have any interesting factorisation properties at the points in the Coulomb branch at which the quadratic differential becomes Strebel and the edge lengths of the ribbon graph are fixed to be equal. Doing so would salvage some connections and parallels with the work of [10, 11]. More generally, it would be an interesting and worthwhile task to carry out these investigations into Gaiotto theories of higher rank; this is likely to be a fertile and fascinating field for future research.

Acknowledgements

This paper developed out of a fourth year undergraduate MPhys project undertaken by J.R. at the University of Oxford in 2013, under the supervision of Y-H.H. and in correspondence with Diego Rodriguez-Gomez. We are particularly indebted to Diego for his work on earlier drafts of this paper, and for his invaluable insights and comments throughout. We are also grateful to Amihay Hanany and John McKay for helpful guidance, as well as to the anonymous reviewer for insightful comments. Y-H.H. is indebted to the Science and Technology Facilities Council, UK, for grant ST/J00037X/1; the Chinese Ministry of Education, for a Chang-Jiang Chair Professorship at NanKai University; the city of Tian-Jin for a Qian-Ren Award; and Merton College, Oxford for their continued support. J.R. is supported by an AHRC scholarship at the University of Oxford, and is also grateful to Trinity College, Cambridge for a Studentship in Mathematics in 2013/14, and to Merton College, Oxford, for support.

References

- [1] N. Seiberg and E. Witten, “Electric-Magnetic Duality, Monopole Condensation, and Confinement in $\mathcal{N} = 2$ Supersymmetric Yang-Mills Theory,” Nuclear Physics B, 1994.
- [2] Yang-Hui He and John McKay, “ $\mathcal{N} = 2$ Gauge Theories: Congruence Subgroups, Coset Graphs and Modular Surfaces”, Journal of Mathematical Physics 54, 2013.
- [3] A. Hanany and N. Mekareeya, “Tri-vertices and SU (2)s,” Journal of High Energy Physics, vol. 69, no. 2, 2011.
- [4] B. Feng, Y.-H. He, K. Kennaway, and C. Vafa, “Dimer Models from Mirror Symmetry and Quivering Amoebae,” Advances in Theoretical and Mathematical Physics, vol. 12, no. 3, 2008.
- [5] Davide Gaiotto, “ $\mathcal{N} = 2$ Dualities,” Journal of High Energy Physics, vol. 34, no. 8, 2012.

- [6] Davide Gaiotto, Gregory W. Moore and Andrew Neitzke, “Wall-crossing, Hitchin Systems, and the WKB Approximation”, arXiv:0907.3987.
- [7] M. Alim, S. Cecotti, C. Córdova, S. Espahbodi, A. Rastogi, and C. Vafa, “ $\mathcal{N} = 2$ Quantum Field Theories and Their BPS Quivers,” 2011.
- [8] M. Alim, S. Cecotti, C. Córdova, S. Espahbodi, A. Rastogi, and C. Vafa, “BPS Quivers and Spectra of Complete $\mathcal{N} = 2$ Quantum Field Theories,” 2011.
- [9] S. Cecotti and C. Vafa, “Classification of Complete $\mathcal{N} = 2$ Supersymmetric Theories in 4 Dimensions, 2011.
- [10] S. Ashok, F. Cachazo, and E. Dell’Aquila, “Strebel Differentials with Integral Lengths and Argyres-Douglas Singularities,” 2006.
- [11] S. Ashok, F. Cachazo, and E. Dell’Aquila, “Childrens Drawings from Seiberg-Witten Curves,” 2006.
- [12] M. Mulase and M. Penkava, “Ribbon Graphs, Quadratic Differentials on Riemann Surfaces, and Algebraic Curves Defined over $\overline{\mathbb{Q}}$,” Asian Journal of Mathematics, vol. 2, no. 4, 1998.
- [13] Yang-Hui He, John McKay and James Read, “Modular Subgroups, Dessins d’Enfants and Elliptic K3 Surfaces”, LMS Journal of Computation and Mathematics 16:271–318, 2013.
- [14] John McKay, “Graphs, Singularities and Finite Groups,” Proc. Symp. Pure Math. 37, 1980.
- [15] Amihay Hanany and Yang-Hui He, “Non-Abelian Finite Gauge Theories,” J. High Energy Phys. 13, 1999.
- [16] K. Strebel, Quadratic Differentials. No. 5 in A Series of Modern Surveys in Mathematics, Springer, 1984.
- [17] Ernesto Gironde and Gabino Gonzalez-Diez, “Introduction to Compact Riemann Surfaces and Dessins d’Enfants,” London Mathematical Society Student Texts 79, Cambridge University Press, 2012.

- [18] Pierre Lochak and Leila Schneps (eds.), “Geometric Galois actions 1”. London Mathematical Society Lecture Note Series, 242, Cambridge University Press (1997).
- [19] Pierre Lochak and Leila Schneps (eds.) “Geometric Galois actions 2”. London Mathematical Society Lecture Note Series, 243, Cambridge University Press (1997).
- [20] Leila Schneps (ed.), “The Grothendieck theory of dessins denfants”. London Mathematical Society Lecture Note Series, 200, Cambridge University Press (1994).
- [21] G. A. Jones and D. Singerman, “Belyi functions, hypermaps and Galois groups”. Bull. London Math. Soc. 28:6, 1996, 561-590.
- [22] J. McKay and A. Sebbar, “J-invariants of arithmetic semistable elliptic surfaces and graphs’, Proceedings on Moonshine and related topics, Montréal, QC, 1999, CRM Proceedings and Lecture Notes 30 (American Mathematical Society, New York, 2001) 119-130.
- [23] Edray Goins, “Dessin Explorer” Mathematica Notebook, 2012, <http://www.math.purdue.edu/~egoins/site//Dessins%20d%27Enfants.html>.
- [24] Nicolas Magot and Alexander Zvonkin, “Belyi Functions for Archimedean Solids”, Discrete Mathematics 217, 2000.
- [25] Melanie Wood, “Belyi-Extending Maps and the Galois Action on Dessins d’Enfants”, Publ. RIMS, Kyoto Univ. 42 (2006), 721-737.
- [26] Yuji Tachikawa, “ $\mathcal{N} = 2$ Supersymmetric Dynamics for Pedestrians”, 2014, arXiv:1312.2684v2.
- [27] R. C. Read, “Some enumeration problems in graph theory,” Ph.D. dissertation, University of London, 1958.
- [28] R. W. Robinson, “Counting cubic graphs,” Journal of Graph Theory 1, 1977.
- [29] R. W. Robinson and N. C. Wormald, “Numbers of cubic graphs,” Journal of Graph Theory 7, 1983.
- [30] Vishnu Jejjala, Sanjaye Ramgoolam and Diego Rodriguez-Gomez, “Toric CFTs, Permutation Triples, and Belyi Pairs,” Journal of High Energy Physics 65, 2011.

- [31] O. Aharony, A. Hanany and B. Kol, “Webs of (p,q) five-branes, five-dimensional field theories and grid diagrams,” JHEP 9801, 002 (1998) [hep-th/9710116].
- [32] Luis F. Alday, Davide Gaiotto and Yuji Tachikawa, “Liouville Correlation Functions from Four-dimensional Gauge Theories”, Letters in Mathematical Physics 91, 2010.
- [33] A. Brandhuber, N. Itzhaki, J. Sonnenschein, S. Theisen and S. Yankielowicz, “On the M theory approach to (compactified) 5-D field theories,” Phys. Lett. B 415, 127 (1997) [hep-th/9709010].
- [34] E. Witten, “Solutions of four-dimensional field theories via M theory,” Nucl. Phys. B 500, 3 (1997) [hep-th/9703166].
- [35] Fritz Beukers and Hans Montanus, “Explicit calculation of elliptic fibrations of K3-surfaces and their Belyi-maps,” Number theory and polynomials, 33–51, LMS Lecture Note Series, 352, CUP, 2008.